

Cite this article as: Rare Metal Materials and Engineering, 2020, 49(12): 4112-4120.

ARTICLE

Effect of Ce on Rolling Microstructure and Tensile Properties of FH40 Shipbuilding Steel Plate

Meng Xianghai^{1,2}, Wang Zhe¹, Wang Meng², Li Mengxing³, Li Yungang¹

¹ College of Metallurgy and Energy, North China University of Science and Technology, Tangshan 063210, China; ² Tangshan Polytechnic College, Tangshan 063299, China; ³ HBIS Group Tangshan Iron Co., Ltd, Tangshan 063016, China

Abstract: FH40 experimental steel with different Ce contents was prepared by vacuum induction furnace. The rolling microstructure of the steel was observed by OM, SEM, TEM and EDS, and its tensile properties and fracture morphology were tested and analyzed. The influence mechanism of Ce on the rolling microstructure and tensile properties of FH40 steel was studied. The results show that with the increase of Ce content from 0 to 0.058wt%, the rolling microstructure of the steel is refined. The rolling microstructure changes from polygonal ferrite to fine equiaxed ferrite, with the formation of granular bainite. The composite inclusions of Ce-O-S+TiN and Ce-O-S are produced in the steel containing 0.0273wt% Ce and 0.058wt% Ce, with four and five pieces of intragranular acicular ferrite (IAF) induced, respectively. The yield strength and tensile strength of the experimental steel containing 0.058wt% Ce are 31 MPa and 33 MPa higher than those of the experimental steel without Ce, respectively. The experimental steels show dislocation strengthening and second phase strengthening. The precipitates in the experimental steel without Ce are mainly the composite phase of Nb-Ti. Nb-Ti-Ce is the main composite phase in the experimental steel containing 0.058wt% Ce, and it is more dispersive and finer with higher dislocation density. The fracture morphology is more uniform. The dimple becomes larger and deeper, which makes it more difficult to fracture under the action of shear stress, thus improving the tensile strength of steel.

Key words: FH40 steel; rolling microstructure; Ce content; acicular ferrite; second phase strengthening

With the rapid development of China's shipbuilding industry, shipbuilding steel plate is developing towards lightweight. The demand for shipbuilding steel plate with high strength and excellent low temperature impact toughness is growing. Therefore, all countries are trying to develop low alloy shipbuilding steel plate with high strength and excellent weldability. In order to improve the production efficiency, the large line energy welding above 50 kJ/cm is widely applied. However, the performance of heat affected zone (HAZ) will inevitably deteriorate because of the increase of line energy, then affecting the overall mechanical properties of shipbuilding steel plate. Therefore, to improve the comprehensive performance of shipbuilding steel plate by reducing carbon content and carbon equivalent of steel plate, control of HAZ grain size of original austenite, HAZ structure of oxide metallurgy, structure transformation of heat affected

zone, etc, have been widely studied^[1-4]. Microalloying is an important way to improve steel's microstructure and toughness. In the smelting process, Nb, V, Ti, Zr and other elements are added, generally less than 0.10wt%, and they are combined with carbon and nitrogen to synthesize carbide, nitride and carbonitride. At high temperature, the growth of original austenite grains is hindered, and the growth of recrystallized grains is inhibited. Original austenite grains play a role of precipitation strengthening at low temperature^[5,6]. In recent years, rare earth elements play an important role in improving the mechanical properties of steel due to their special physical and chemical properties. Therefore, the addition of rare earth elements has become a new trend in the composition design of offshore steel^[7,8].

In this research, FH40 shipbuilding steel plate with different Ce content was prepared by vacuum induction melting furnace.

Received date: April 19, 2020

Foundation item: National Natural Science Foundation of China (51974129); Natural Science Foundation of Hebei Province (E2020105187)

Corresponding author: Li Yungang, Ph. D., Professor, College of Metallurgy and Energy, North China University of Science and Technology, Tangshan 063210, P. R. China, Tel: 0086-315-8832175, E-mail: lyg@ncst.edu.com

Copyright © 2020, Northwest Institute for Nonferrous Metal Research. Published by Science Press. All rights reserved.

The effect of trace Ce on the rolling microstructure, fracture morphology and strengthening mechanism of FH40 shipbuilding steel plate was studied. And the effect of cerium inclusion particles on the induction of intragranular acicular ferrite (IAF) was studied. The research provides a theoretical basis for the preparation of new FH40 shipbuilding steel plate with excellent structure and properties by alloying.

1 Experiment

1.1 Smelting process

The experimental steel was smelted in a 50 kg vacuum induction furnace. The main raw materials include industrial pure iron, carbon powder, ferrosilicon, manganese, aluminum, cerium, zirconium, etc. Part of the cold material was put into the furnace, and the vacuum degree in the furnace was controlled below 6.67×10^{-2} Pa. After the material was melted for 5 min, ferroniobium was added. Standing for 1 min, carbon, ferrosilicon and manganese were added successively. After the melting was completed, aluminum was added. After all the alloys were melted, argon was filled into the furnace to keep the furnace pressure at -0.07 MPa. Zr was added to the liquid surface through the bin. The cerium block was wrapped with pure iron sheet, and inserted into the bottom of the liquid metal. The mixture was stirred for 1 min, and then poured. The ingot taken out was a cylinder, with a circle of $\varnothing 150$ mm at the bottom and a height of 170 mm. The metal materials melted by this method have uniform structure and high density^[9]. There are three types of experimental steel, including FH40 base steel (F1), FH40 experimental shipbuilding steel plate with 0.0273wt% cerium (F2) and FH40 experimental shipbuilding steel plate with 0.058wt% cerium (F3).

1.2 Composition of smelting steel

Ingot sample was taken for composition analysis. The test result is shown in Table 1. The mass fraction of Si, Mn, Ni, Nb, Ti, Al, P, Cr, Mo, V and other elements was measured by direct reading spectrometer. The mass fraction of C and S elements was measured by CS-800 infrared carbon sulfur analyzer. Mass fraction of O and N elements was measured by TCH600 nitrogen/oxygen/hydrogen determinator. The mass fraction of Ce was measured by inductively coupled plasma-atomic emission spectrometry (ICP-AES).

It can be seen that the experimental smelting steel is within the required composition range compared with the composition range of FH40 shipbuilding steel plate provided by a steel plant^[10].

1.3 Forging and rolling

The smelted sample was taken out and forged into slab by 750 kg air hammer. The forging process was as follows: The heating temperature was 1200 °C. The holding time was 40 min. The open forging temperature was 1150 °C. The final forging temperature was 900 °C. The terminal size was 100 mm×100 mm×300 mm. And the cooling method was air cooling.

The forged slab was rolled by 550 double high reversing rolling mill. The rolling process was as follows: the forging was heated to 1200 °C for 2 h. The rolling process was divided into rough rolling and finish rolling. The start rolling temperature of rough rolling was 1150 °C, and the finish rolling temperature of rough rolling was ≥ 1000 °C. It came out 50% deformation after three times of rough rolling. It came out 70% deformation after four times of finish rolling. And the finish rolling temperature was controlled at 890 °C. The cooling speed was 10 °C/s, then air cooling was proceeded.

1.4 Research methods

The metallographic specimen with the size of 10 mm×10 mm×5 mm was cut at 1/4 width of the steel plate. The polished metallographic specimen was corroded with 4% nitric acid alcohol solution for 20~30 s. And the rolling microstructure was obtained. The rolling microstructure was analyzed by Axiovert200 ZEISS metallographic microscope and Sigma 500 field emission scanning electron microscope (FESEM).

The tensile sample was taken along the rolling direction of steel plate according to GB/T2975. According to GB/T228.1-2010, Metallic Materials Tensile Test: tensile test method at room temperature, test was performed by INSTRON-3382 electronic universal tensile testing machine. The experimental temperature was 20 °C. The tensile rate was 0.45 mm/min. And the test error was less than 2%. The engineering stress-strain curve can be obtained. The tensile strength R_m and elongation A of the sample can be obtained. And the average value of three tests was used as the final result. After the experiment, field emission scanning electron microscope (Sigma 500) and field emission gun transmission electron microscope (FEI Tencnai G2 F20) were used to observe the fracture surface and to analyze the fracture and strengthening mechanism.

2 Results and Discussion

2.1 Rolling microstructure of FH40 shipbuilding steel plate

2.1.1 Rolling microstructure

Fig.1a shows that the base steel is composed of polygonal ferrite (PF), a small amount of bainite (B) and chain pearlite

Table 1 Chemical composition of F1~F3 experimental steel (wt%)

Steel	C	Si	Mn	P	S	Cr	Mo	Ni	Al	Nb	Ti	V	Ce	O	N
F1	0.0673	0.250	1.59	0.0096	0.0072	0.110	0.0492	0.349	0.0160	0.0395	0.0277	0.0522	0	0.0364	0.0078
F2	0.0665	0.239	1.56	0.0099	0.0057	0.115	0.0429	0.330	0.0702	0.0440	0.0212	0.0525	0.0273	0.0231	0.0067
F3	0.0701	0.225	1.54	0.0097	0.0055	0.111	0.0480	0.331	0.0438	0.0555	0.0141	0.0525	0.0580	0.0260	0.0059

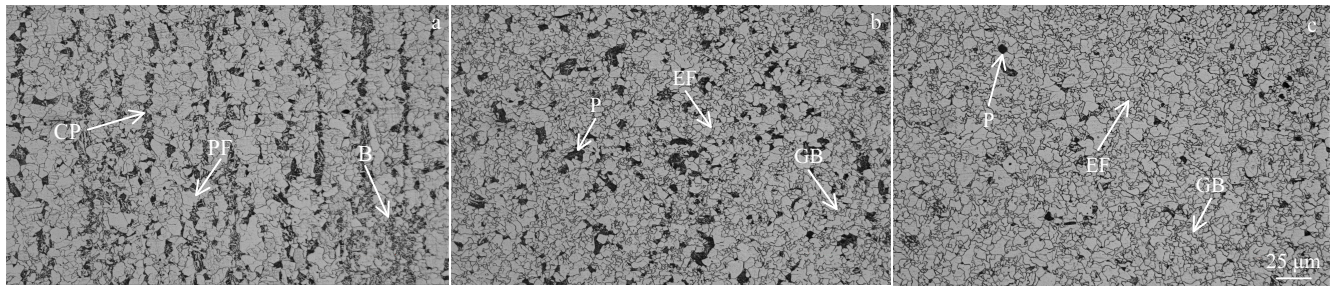


Fig.1 Metallographic rolling microstructure F1 (a), F2 (b), and F3 (c) experimental steel

(CP). When 0.0273wt% Ce is added to the steel, the structure of the steel changes from polygonal ferrite to equiaxed ferrite (EF). And the grain size of ferrite obviously decreases. Fig.1b shows that the chain pearlite disappears and granular bainite (GB) forms. Fig.1c shows that as Ce content in steel increases from 0.0273wt% to 0.058wt%, the grain refinement degree of the rolling microstructure is enhanced, the pearlite content is obviously reduced, and the granular bainite is distributed in dispersion. This is because the total banded structure of F+P in steel is reduced after Ce is added. Rare earth elements can reduce the carbon content of solid solution in austenite, increase the quantity of ferrite and decrease the grain size of ferrite. Meanwhile, Ce interacts with low melting point elements in steel to form rare earth compounds and metal compounds with high melting point in various atomic ratios. These compounds disperse in steel and become the nucleation core, thus refining the grains^[11-13].

2.1.2 Structural characteristics of IAF in the rolling microstructure

Fig.2 is the rolling microstructure and EDS spectrum of typical inclusions of F1 experimental steel. It can be seen that the inclusion particle is a composite phase of Al-O+MnS+TiN, which is nearly rectangle in shape. In addition to polygonal ferrite, granular bainite is also distributed. The granular bainite is usually formed around the ferrite, which is the transformation product of undercooled austenite at medium temperature and plays the role of second phase strengthening in steel. As the granular bainite is isotropic and its shape is close to spherical, it plays a strengthening role in steel. Therefore, the fine and dispersed granular bainite is beneficial to refine the structure and to improve the mechanical properties of the steel^[14,15].

Fig.3 shows the EDS mapping of composite phase of inclusions in steel. The inclusion is rectangular in shape and about 2.5 μm×3.4 μm in size. It mainly consists of three parts: Al-O as the core, MnS on the left side and TiN on the right side. They uniformly wrap Al-O, and no IAF is found.

Fig.4 shows the SEM morphology and EDS spectrum of typical inclusions of the rolled F2 experimental steel. It can be seen that the inclusion particle is a composite phase of

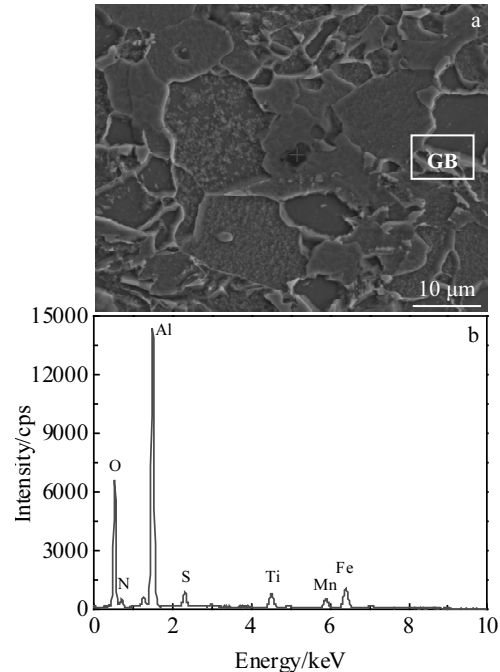


Fig.2 SEM image (a) and EDS spectrum (b) of typical inclusions in rolling microstructure of F1 experimental steel

Ce-O-S+TiN, which is nearly spherical in shape and about 2.3 μm in size. Based on the inclusion, four pieces of IAF (a1, a2, a3, a4) are induced, and the angle between two adjacent pieces of IAF is about 90°. The composite inclusions of Ce can promote the nucleation of IAF and induce acicular ferrite and refine the grains.

Fig.5 shows the EDS mapping of composite phase of the inclusion. Ce, O and S are evenly distributed, and the formed TiN is located at the boundary.

Fig.6 is the EDS spectrum of typical inclusions in the rolling microstructure of F3 experimental steel. Fig.7 shows the EDS mapping of composite phase of the inclusion. It can be seen that the inclusion particle is a composite phase of Ce-O-S, and its shape is also close to the sphere, with a size of about 1.6 μm. Five pieces of IAF (a1, a2, a3, a4, a5) are induced by the

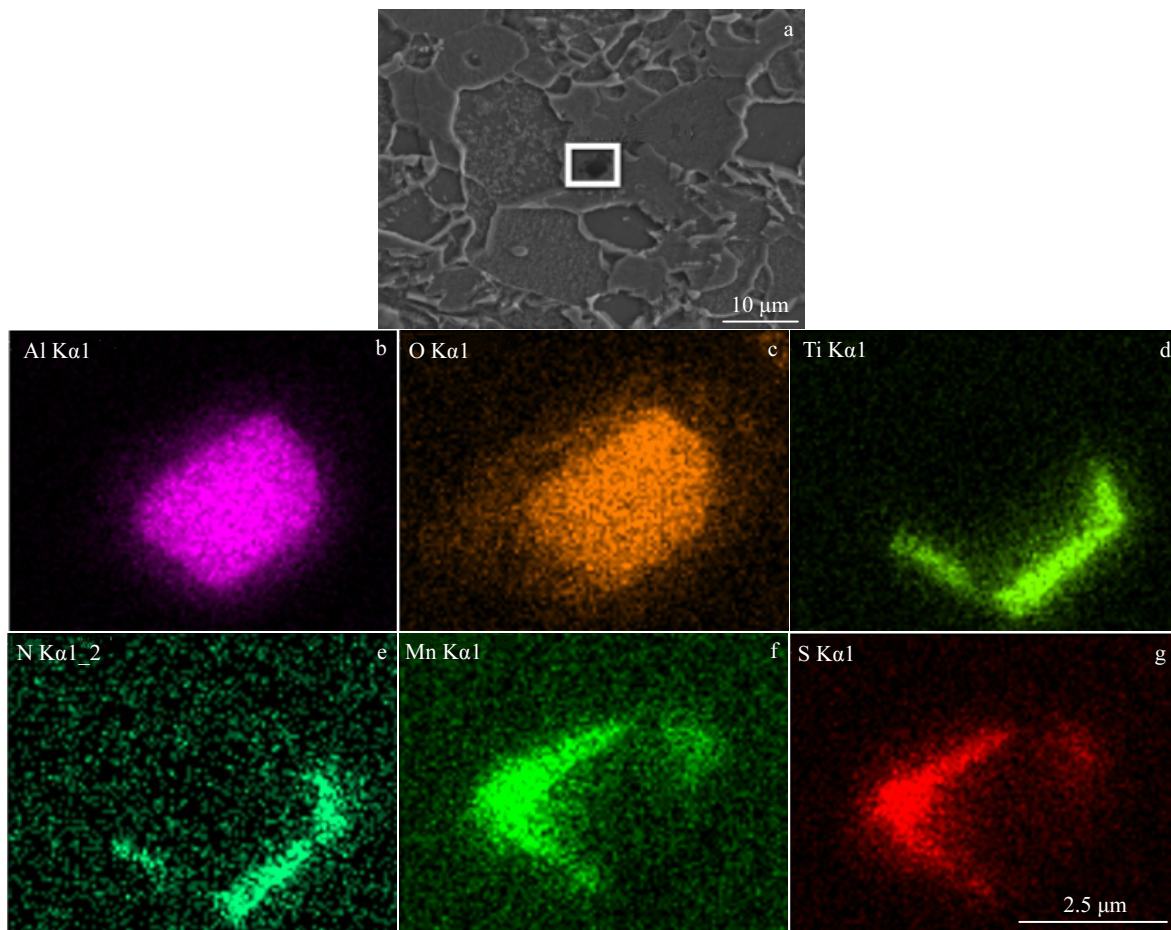


Fig.3 SEM image (a) and EDS mapping (b~g) of composite phase in F1 experimental steel

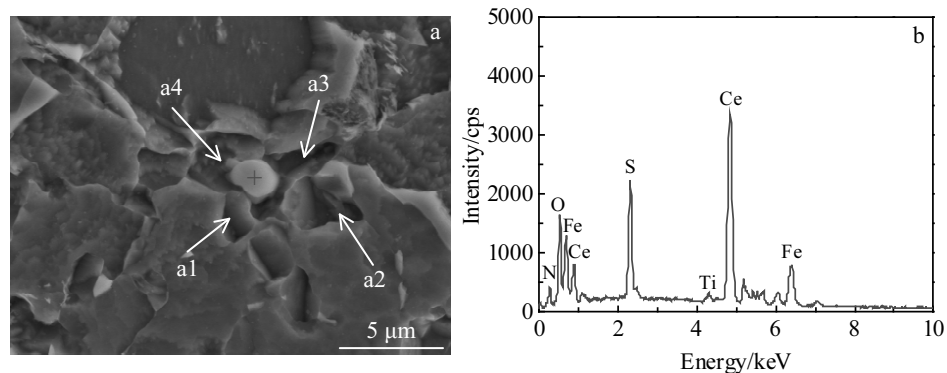


Fig.4 SEM image (a) and EDS spectrum (b) of typical inclusions in as-rolled microstructure of F2 experimental steel

inclusion as the core, and a4 which is near to the right side grows more sufficiently. Compared with Fig.4, due to the increase of IAF number, the grains can be refined better^[16]. Thewlis^[17] found that rare earth element Ce can react with S in steel to form rare earth oxides and sulfides, and precipitate continuously during cooling and solidification, showing fine dispersion distribution. They have a good mismatch with α -Fe,

which can effectively promote the heterogeneous nucleation of acicular ferrite. This discovery fits well with the principle of minimum mismatch.

2.2 Tensile properties of FH40 shipbuilding steel plate

2.2.1 Tensile test

Table 2 shows the mechanical property requirements of FH40 shipbuilding steel plate from International Association of

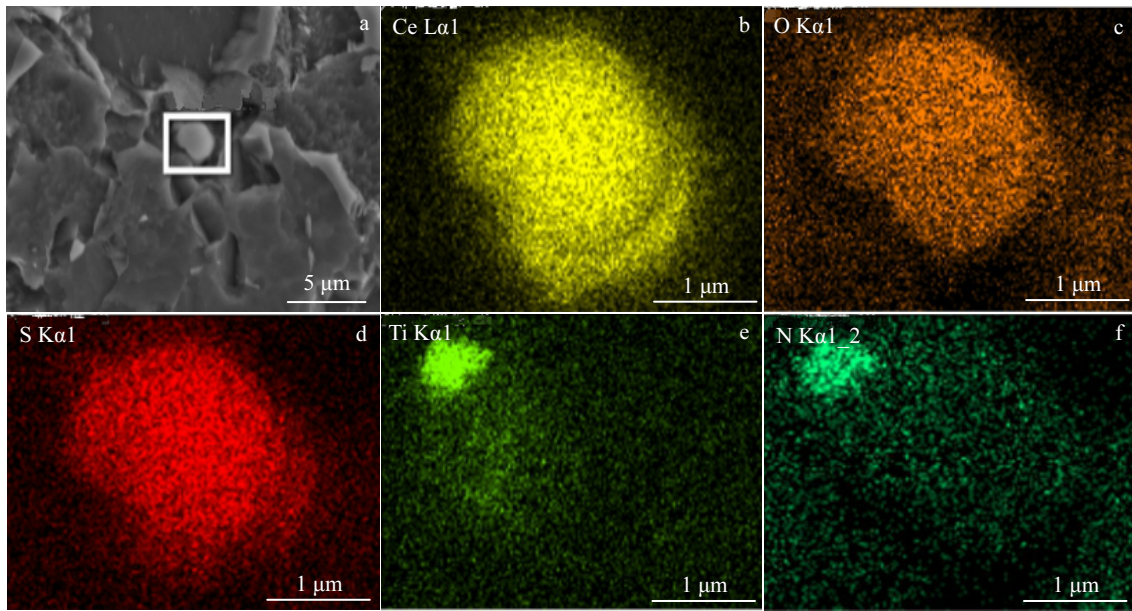


Fig.5 SEM image (a) and EDS mapping (b~f) of composite phase in F2 experimental steel

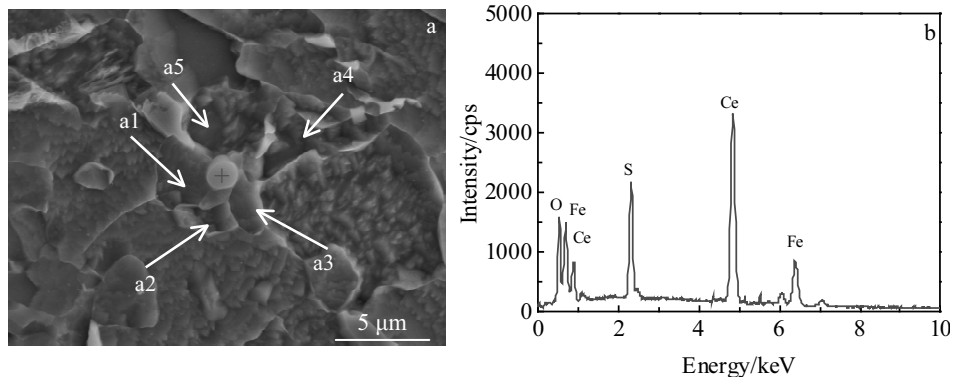


Fig.6 SEM image (a) and EDS spectrum (b) of typical inclusions in the rolling microstructure of F3 experimental steel

Classification Societies^[18]. Table 3 shows the test results of the tensile properties of F1~F3 experimental steel. The yield strength, tensile strength, elongation and low-temperature impact energy after fracture of F1~F3 are compared. The mechanical properties of F1~F3 meet the requirements in Table 2.

It can be seen from Table 3 that the yield strength and tensile strength of the Ce treated steel plate are superior to those of the base steel, because the rolling microstructure is refined and the inclusion induces IAF in the steel. Low yield strength ratio means that the material is easy to plastic deformation under the action of external force and will not fracture easily. High yield strength ratio indicates that the material has high hardness, strong deformation resistance and is not prone to plastically deform, but it will fracture soon after deformation. It is generally believed that if the yield

strength ratio of steel is lower than 0.85, the safety and stability of shipbuilding steel plate can be ensured^[19]. It can be seen from Table 3 that the yield strength ratios of the experimental steels are all about 0.72, which indicate that the steels have excellent plastic deformation, and are not prone to fracture. Meanwhile, the longitudinal and transverse impact energy of F2 and F3 experimental steel that is added with Ce increase compared with those of F1 experimental steel. The longitudinal impact energy of F2 and F3 experimental steel increases from 117.0 J to 150.5 and 190.3 J, increased by 28.6% and 62.6%, respectively. The transverse impact energy increases from 74.7 J to 101.8 and 124.8 J, increased by 36.2% and 67.1%, respectively. The addition of Ce can refine the grains and promote the nucleation of IAF, thus improving the low-temperature impact toughness of the experimental steel.

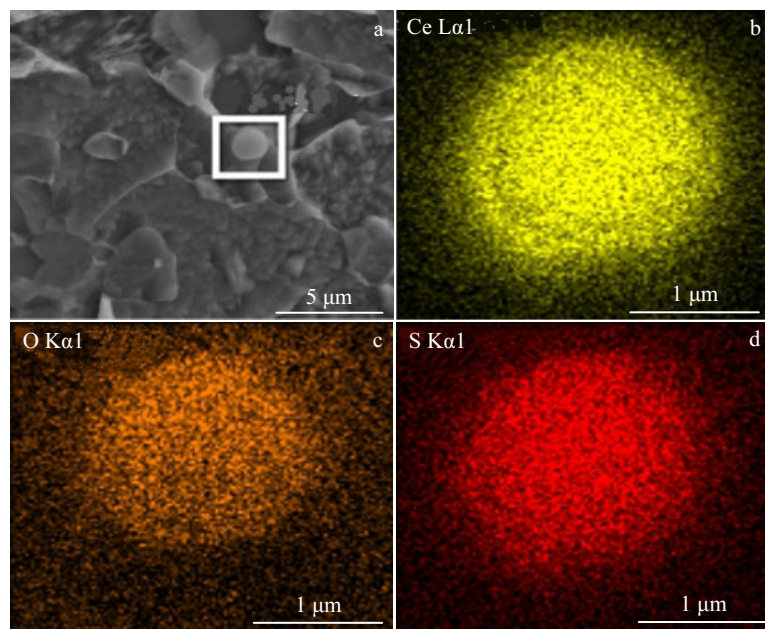


Fig.7 SEM image (a) and EDS mapping (b~d) of composite phase in F3 experimental steel

Table 2 Mechanical properties of FH40 shipbuilding steel plate^[18]

Steel	Tensile test			Impact temperature/ °C	V type impact experiment	
	Yield strength, R_{el}/MPa	Tensile strength, R_m/MPa	Elongation after fracture, $A/%$		Impact energy, α_k/J Longitudinal	Transverse
FH40	≥390	510~660	≥20	-60	≥41	≥27

Table 3 Tensile test results of F1~F3 experimental steel

Steel	Yield strength, R_{el}/MPa	Tensile strength, R_m/MPa	Yield ratio	Elongation after fracture, $A/%$	Impact Energy (-60 °C), α_k/J Longitudinal	Transverse
F1	426	589	0.72	22.0	117.0	74.7
F2	433	605	0.72	22.8	150.5	101.8
F3	457	622	0.73	22.2	190.3	124.8

Fig.8 shows the tensile engineering stress-strain curve of F1~F3 experimental steel at room temperature. Fig.8 shows that except the F1 experimental steel, the F2 and F3 experimental steel continuously yield, and there is no obvious yield platform. When the elongation of steel is 14%, 16% and 14%, the maximum tensile strength is 589, 605 and 622 MPa. When Ce content is 0.0273wt% and 0.058wt%, the yield strength of the steel is 433 and 457 MPa, respectively, which is 7 and 31 MPa higher than that of F1 experimental steel; the tensile strength of the steel is 605 and 622 MPa, increased by 16 and 33 MPa compared to that of F1 steel, respectively. Ce has a strong deoxidizing and desulfurizing effect, which can form Ce_2O_3 and Ce_3S_4 , reduce the content of sulfur and oxygen, eliminate the formation of Al_2O_3 clusters, and inhibit the segregation of manganese at the grain boundary, thus strengthening the grain boundary, improving the quality of the grain boundary, and significantly improving the

tensile strength^[16]. The elongation of experimental steel after fracture meets the requirements of International Association of

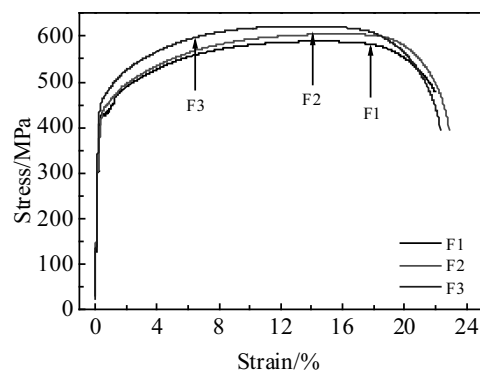


Fig.8 Tensile engineering stress-strain curves at room temperature

Classification Society. In the aspect of elongation, $F2 > F3 > F1$, which may be related to the change of strengthening mechanism with the increase of Ce content.

2.2.2 Tensile fracture morphology

Fig.9a shows the uneven fracture morphology of F1 experimental steel, in which the dimple is small and shallow, the diameter is large and the number of deeper dimple is small. And there are irregular inclusions in the dimple. Fig.9b shows the fracture morphology of F2 experimental steel. Compared with the F1 experimental steel, the fracture morphology of the dimple is more uniform, and the dimple is obviously larger and deeper, showing an equiaxed dimple. And there are irregular inclusions in the dimple. Fig.9c shows the fracture morphology of F3 experimental steel. Like F2 experimental steel, the number of larger and deeper dimples increases. And many small spherical inclusions are distributed in dimples. This shows that the steel has obvious plastic deformation before fracture. Spherical inclusions are more difficult to fracture under the action of shear stress, which is the reason why steel has high tensile strength. The size and depth of dimple are related to the ductility of materials, while the shape of dimple is related to the applied stress. Generally speaking, if the dimple is larger and deeper, the plastic deformation of steel will be sufficient and the corresponding toughness will be better. The small, shallow or even absent dimples indicate that the plastic deformation is insufficient and the toughness is worse.

2.2.3 Strengthening mechanism

To explore the strengthening mechanism of Ce content on FH40 steel, the rolling microstructure of F1 and F3 experimental steels is analyzed by TEM. Fig.10 and Fig.11 show the morphology and element distribution of precipitated phase in F1 and F2 experimental steel, respectively. Due to the small size of precipitates, it is possible to hit the matrix when using point scanning to analyze the composition of precipitates. Therefore, the composite phase in the selected area of steel is scanned to determine the type of composite phase. Fig.10 shows that the typical precipitates in F1 experimental steel is Nb-Ti composite phase with a size of about 34 nm. Due to the low atomic mass of C and N, it is

difficult to accurately calibrate the content of C and N in the precipitates, so the surface scanning map of C and N are not given.

Misra^[20] studied the precipitates in steel and found that the precipitates containing Ti are mainly square and the precipitates containing Nb are mainly spherical. On the basis of solid solution strengthening of C and Mn, Nb and Ti microalloying elements hinder the growth of original austenite grains during heating, inhibit recrystallization and grain growth after recrystallization during rolling, and play a role of precipitation strengthening at low temperature^[21]. The Nb-Ti composite in this research tends to be spherical. As shown in Fig.11, when Ce is added to the steel, the precipitates in F3 experimental steel is a composite phase of Nb-Ti-Ce, with smaller size and more uniform distribution.

Fig.12 is two typical TEM images of the rolling microstructure of F1 experimental steel. Fig.12 shows that in F1 experimental steel, there are high density dislocation lines in ferrite grains near the precipitates. And some dislocation lines in the steel are intertwined, which play a role of dislocation strengthening. The precipitates effectively block the dislocation movement and play the role of second phase strengthening.

Fig.13 is two typical TEM images of the rolling microstructure of F3 experimental steel. Fig.13 shows that the dislocation density in ferrite grains of Ce-treated steel is high. There are a large number of dislocation lines, which intertwine with each other and produce dislocation walls. At this time, dislocation cell, dislocation segregation at grain boundary and a few dislocation grids appear. Because the mesh structure is relatively stable, the pull force and repulsion force between dislocations hinder the movement of dislocations and increase the elastic stress. Such dislocation configuration is very beneficial to resist micro plastic deformation, and the effect of dislocation strengthening is better than that of F1 experimental steel. A large number of fine precipitates dispersed in the steel also hinder the movement of dislocations and play a strong role in strengthening the second phase.

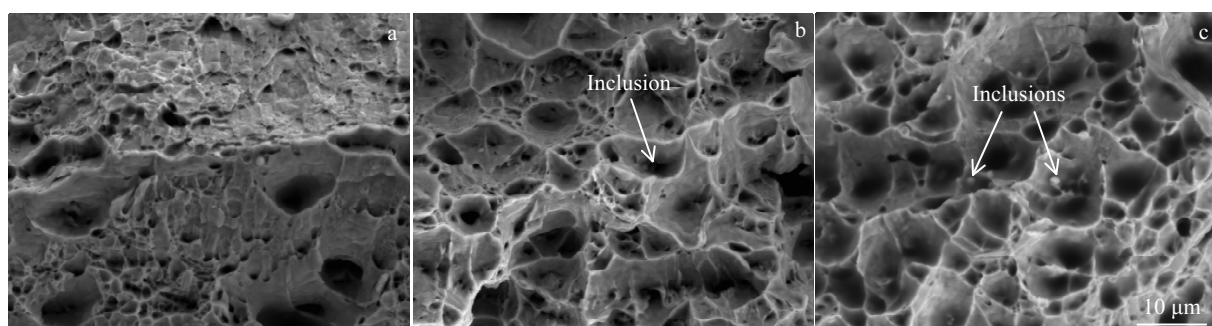


Fig.9 Tensile fracture morphologies of F1 (a), F2 (b), and F3 (c) experimental steel

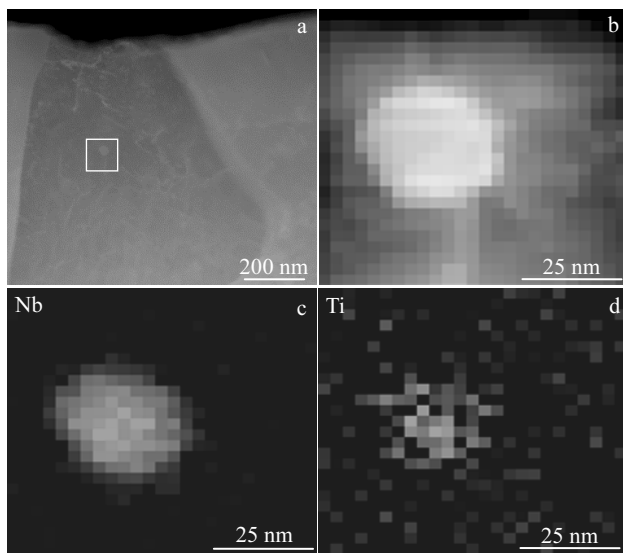


Fig.10 Morphologies (a, b) and element distributions (c, d) of typical precipitates in F1 experimental steel

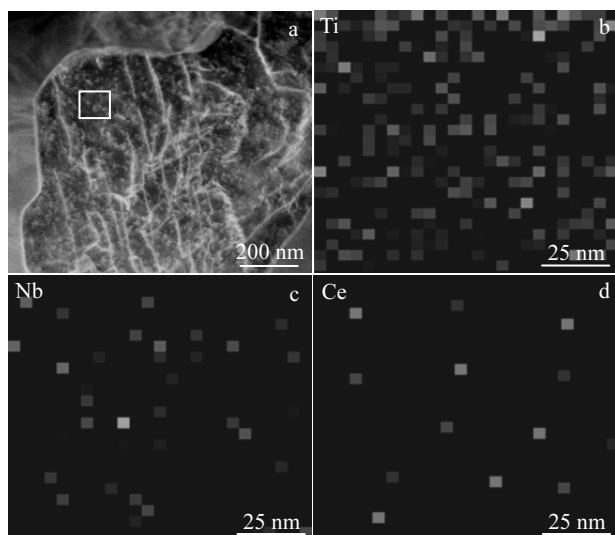


Fig.11 Morphology (a) and element distributions (b-d) of precipitated phase in F3 experimental steel

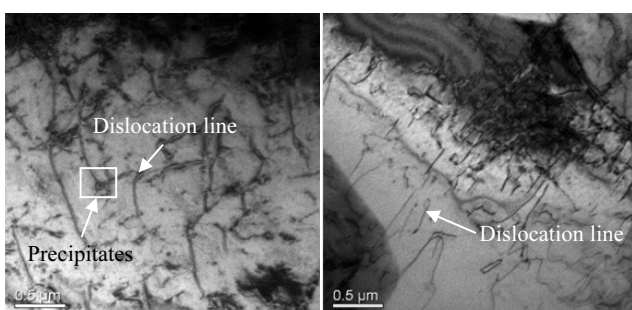


Fig.12 TEM images of typical rolling microstructure in F1 experimental steel

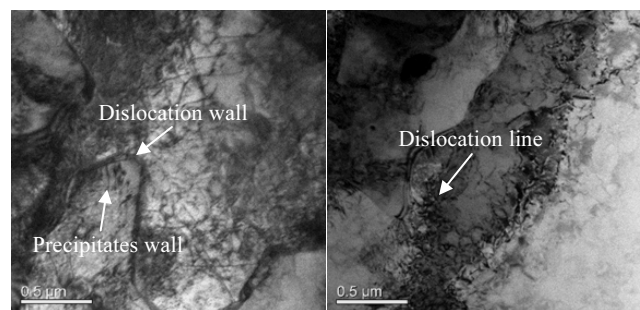


Fig.13 TEM images of rolling microstructure in F3 experimental steel

3 Conclusions

1) After the addition of 0.0273wt% and 0.058wt% Ce, the microstructure changes from strip ferrite to equiaxed ferrite, the ferrite grains become smaller, the shape of bainite becomes granular, and the microstructure is refined. Intragranular acicular ferrite (IAF) is not induced by Al-O compound inclusions in FH40 experimental steel without Ce addition. The composite inclusions of Ce-O-S+TiN in the steel containing 0.0273wt% Ce induce 4 pieces of IAF, and the composite inclusions of Ce-O-S in the steel containing 0.058wt% Ce induce 5 pieces of IAF.

2) Compared to the steel without Ce addition, the yield strength of the experimental steel with 0.0273wt% Ce and 0.058wt% Ce increases by 7 and 31 MPa, respectively, and the tensile strength increases by 16 and 33 MPa, respectively. The elongation to fracture increases to some extent, and the elongation reaches the highest (22.8%) when the content of Ce is 0.0273wt%.

3) The experimental steels all present dislocation strengthening and second phase strengthening. The precipitates in the FH40 experimental steel is mainly Nb-Ti composite phase. The experimental steel containing 0.058wt% Ce mainly consists of Nb-Ti-Ce composite phase, which is more dispersive and finer, with higher dislocation density. The fracture morphology of steel after Ce treatment is more uniform, and the dimple changes from small and shallow to large and deep, which makes it more difficult to fracture under the action of shear stress, thus improving the tensile strength of steel.

References

- 1 Zhao Jie. *Materials Reports*[J], 2018(S1): 428 (in Chinese)
- 2 Xu Longyun, Yang Jian, Wang Ruizhi et al. *Journal of Iron and Steel Research International*[J], 2018, 25(4): 433
- 3 Yamamoto K, Hasegawa T, Takamura J. *ISIJ International*[J], 1996, 36(1): 80
- 4 Wang Ruizhi, Yang Jian, Xu Longyun. *Metals*[J], 2018, 8(11): 946

5 Luo Xingzhuang, Yuan Qinpan, Yang Yuebiao et al. *Wide and Heavy Plate*[J], 2018, 24(6): 14 (in Chinese)

6 Xiang Yong, Chen Zhiguo, Wei Xiang et al. *Rare Metal Materials and Engineering*[J], 2015, 44(6): 1335 (in Chinese)

7 Shigesato G, Sugiyama M, Aihara S et al. *Journal of the Iron and Steel Institute of Japan*[J], 2001, 87(2): 93

8 Chai Feng, Su Hang, Yang Caifu et al. *Journal of Iron and Steel Research, International*[J], 2014, 21(3): 369

9 Xue Zhengliang, Li Zhengbang, Zhang Jiawen et al. *Journal of Iron and Steel Research*[J], 2003, 15: 5

10 State Administration for Market Regulation. *Ship and Offshore Engineering Steel for Low Temperature Service*, GB/T 37602-2019[S], 2019 (in Chinese)

11 Yang Jichun, Yu Haicun, Gao Jianjun. *Chinese Rare Earths*[J], 2015, 36(5): 43 (in Chinese)

12 Zhang Pengyan. *Research and Application of Microstructure Control Technology for Large Heat Input Welding*[M]. Beijing: Metallurgical Industry Press, 2014: 106 (in Chinese)

13 Chen Shaohua, Mi Xujun, Bie Lifu et al. *Rare Metal Materials and Engineering*[J], 2020, 49(3): 811

14 Li Xiaobing. *Thesis for Doctorate*[D]. Shenyang: Northeastern University, 2016 (in Chinese)

15 Cui Zhongqin, Tan Yaochun. *Metallography and Heat Treatment*[M]. Beijing: China Machine Press, 2007: 87 (in Chinese)

16 Jiang M Z, Yu Y C, Li H et al. *High Temperature Materials and Processes*[J], 2017, 36(2): 145

17 Thewlis G. *Materials Science and Technology*[J], 2006, 22(2): 153

18 China Classification Society. *Rules For Materials and Welding*[M]. Beijing: China Communications Press, 2016: 7 (in Chinese)

19 Qi Jianghua, Xue Zhengliang, Wu Jie et al. *Iron & Steel*[J], 2010, 45(5): 33 (in Chinese)

20 Misra R D K, Weatherly G C, Hartmann J E et al. *Materials Science and Technology*[J], 2001, 17(9): 1119

21 Wang Youming, Li Manyun, Wei Guang. *Control Rolling and Cooling of Steel*[M]. Beijing: Metallurgical Industry Press, 1995: 51 (in Chinese)

Ce 对 FH40 船板钢轧态组织及拉伸性能的影响

孟祥海^{1,2}, 王 哲¹, 王 萌², 李孟星³, 李运刚¹

(1. 华北理工大学 冶金与能源学院, 河北 唐山 063210)

(2. 唐山工业职业技术学院, 河北 唐山 063299)

(3. 河钢集团唐钢公司, 河北 唐山 063016)

摘要: 利用真空感应炉制备不同 Ce 含量的 FH40 实验钢, 采用 OM、SEM、TEM 和 EDS 手段观察钢的轧态组织, 并对其拉伸性能和断口形貌进行测试与分析, 研究了 Ce 对 FH40 钢轧态组织以及拉伸性能的影响机制。结果表明, 随着 Ce 含量从 0 增加到 0.058% (质量分数, 下同), 钢的轧态组织得到细化, 由多边形铁素体变为细小的等轴状铁素体, 同时出现粒状贝氏体; 含 0.0273% Ce 和 0.058% Ce 钢中分别产生了 Ce-O-S+TiN 和 Ce-O-S 复合夹杂物, 并且分别诱发了 4 条和 5 条晶内针状铁表体 (IAF)。含 0.058% Ce 实验钢的屈服强度、抗拉强度较基体钢分别提高了 31、33 MPa。当 Ce 含量为 0.0273% 时实验钢的延伸率达到了 22.8%。实验钢均表现为位错强化和第二相强化, 基体钢中析出相主要是 Nb-Ti 的复合相, 含 0.058% Ce 实验钢中主要是 Nb-Ti-Ce 的复合相, 且更加弥散细小, 位错密度更高; 同时断口形貌更加均匀, 韧窝由小而浅转变为大而深, 使其在切应力的作用下更不易断裂, 因而提高了钢材的抗拉强度。

关键词: FH40 钢; 轧态组织; Ce 含量; 针状铁素体; 第二相强化

作者简介: 孟祥海, 男, 1983 年生, 博士, 副教授, 华北理工大学冶金与能源学院, 河北 唐山 063210, 电话: 0315-8832175, E-mail: xianghaimeng@163.com